FRACTAL ANALYSIS OF STOCK EXCHANGE INDICES IN TURKEY

by

Engin Kandıran

B.S., Physics, Boğaziçi University, 2013

Submitted to the Institute for Graduate Studies in
Science and Engineering in partial fulfillment of
the requirements for the degree of
Master of Science

Graduate Program in Computational Science and Engineering
Boğaziçi University
2015

ACKNOWLEDGEMENTS

I would like to express my gratitude to my co-supervisor Prof. Avadis S. Hacınlıyan for his never ending support and guidance to me throughout my M.S. studies. In addition to this I need to mention the patience and understanding of my supervisor Assoc. Prof.Kunt Atalık during this study.

I owe a lot to my family who always trust in me and my decisions about my career and give never ending support in all situations.

This thesis is dedicated to my family to whom I owe everything.

ABSTRACT

FRACTAL ANALYSIS OF STOCK EXCHANGE INDICES IN TURKEY

The purpose of this study is to investigate possible fractal behavior in Istanbul Stock Exchange (BIST) indices. In particular evidence of chaotic and fractal behavior will be presented. To be able to analyze monofractality of given indices we are going to use the Higuchi and Katz methods. In addition to this, we analyze the chaotic behavior of the investigated indices using Rescaled Range Analysis (R/S), Detrended Fluctuation Analysis (DFA) and Power Spectrum (Fourier Transform). To be able to check whether financial time series that we work on are multifractal or not, we apply the well-known methods Multifractal Detrended Fluctuation Analysis (MF-DFA) and Wavelet Transform Modulus Maxima (WTMM). In addition to the analysis of stock market indices, we apply the same analysis to currency closing prices (Euro and Dollar) to check whether their behavior is similar to that of stock market indices or not.

ÖZET

TÜRKİYE'DEKİ BORSA ENDEKSLERİNİN FRAKTAL ANALİZİ

Bu çalışmanın amacı İstanbul Menkul Kıymetler Borsası endekslerindeki muhtemel fraktal davranışları araştırmaktır. Özellikle, kaotik ve fraktal davranışların kanıtları verilecektir. Verilen endekslerin monofraktal davranışlarını analiz etmek için Higuchi ve Katz metodlarını kullanacağız. Buna ek olarak, araştırılan endekslerin kaotik davranışlarını incelemek amacıyla Dönüştürülmüş Genişlik (R/S), Eğilimden Arındırlmış Dalgalanma (DFA) Analizi ve Güç Spekrumu (Fourier Dönüşümü) Analizi kullanılmıştır. İncelediğimiz finansal zaman serilerinin multifraktal (çoklu fraktal) davranış gösterip göstermediğini kontrol etmek için iyi bilinen iki metod kullandık: Multifraktal Eğilimden Arındırılmıs Dalgalanma Analizi (MF-DFA) ve Dalgacık Modül Dönüşüm Maksimumu WTMM. Menkul Kıymetler Borsası endekslerinin analizine ek olarak döviz kapanış fiyatlarına da aynı analizleri uygulayıp, diğer endekslerle benzer davranış gösterip göstermediklerini kontrol etmeye çalıştık.

TABLE OF CONTENTS

LIST OF FIGURES

LIST OF TABLES

1. INTRODUCTION

Humanity has been looking for finding symmetry and smoothness in nature throughout its existence. In general, scientists search for patterns and call the events which do not conform to their conceptual framework as anomalies since these do not match their conceptual framework based on symmetry. However, most of the entities in our physical world do not obey Euclidean geometry at all and exhibit different symmetries.

Through the application of Euclidean geometry to a drawing, we can only create an approximation of a tree. In the real world, trees consist of a network of branches which are very similar to the overall shape of a tree but each branch is different. (Edgar E.Peters, 1994). Furthermore, there are other branches on branches on smaller scales (successive generation of branches). At the individual branch level, each branch has a different size but share certain common properties. This "self-similar" property is one of the features of Fractal geometry. That means the actual structure of a tree includes both local randomness and deterministic point of view.

Another example could be fluid heated from below. Near the source, the fluid is heated by the way of convection. Then the fluid is going to reach an equilibrium state in which maximum entropy occurs. During this heating period, all fluid molecules move independently. When the temperature passes a critical level, molecules which move independently start to behave coherently, that means heat flows by means of convection. In that case, the convection result is known by scientists but direction of roles of molecules is unknown. That means local randomness and global determinism coexist together.

Stock markets are also driven both by microeconomic considerations such as profit levels of firms and macroeconomic considerations such as employment and manufacturing data. The former can be compared to the individual molecules, the latter to the mass action of the molecules.

In that sense, the science of chaos theory and fractals are the places that chance (randomness) and determinism seem together. Economic systems also exhibit complicated dynamic (chaotic) evidences by large amplitude and periodic fluctuation in economic indices, for instance, stock market prices, currency prices,GDP (gross domestic product) (Edgar E.Peters,1994). The classical approach to economic anabolisms is the Newtonian

one in which economic fluctuations are evaluated as linear perturbations near the equilibrium. However, large fluctuations in economic indicators show that economic systems are driven from the equilibrium points such that nonlinearity takes a role and gives the clues of chaotic complex systems.

There are two common hypotheses that try to explain financial markets: Efficient Market Hypothesis and Fractal Market Hypothesis.Efficient Market Hypothesis states that securities markets are efficient, with the prices of securities fully reflecting all available information (Fama, 1991).The idea behind this hypothesis is that "competition will drive all information into the price quickly". According to this hypothesis, if the market is efficient,an investor will be unable to outperform the market consistently. On the other hand,the Fractal Market Hypothesis states that a market consists of many investors, who have different investment horizons and vary in their analysis of information because of their individual time horizons. Fractal Market Hypothesis claims that price changes are due to information being meaningful only to a certain investment segment. This idea is contrary to the Efficient Market Hypothesis. According to the Fractal Market Hypothesis, an equilibrium price does not exist since people value investments differently, while equilibrium in price is possible in the Efficient Market Hypothesis.

In economics stock markets show dynamic structures that can be examined through the use of chaos theory and fractal analysis. The stock market consists of investors from different investment horizons. A stable market is one where all investors can make trade with each other, each confronted with the same risk level as others, adjusted for their investment horizon. However, forecasting using linear approaches to stock market values do not give sufficiently reasonable explanations in many cases.

The laws that govern the variation over prices in financial markets are very complex. The main reason of this complexity in financial markets comes from the interaction among heterogeneous agents and by the interplay of the emerging events in the external environment. These fluctuations in financial markets can be characterized by turbulent features and fractal behavior.

The term "fractal"was first mentioned by the mathematician Benoit Mandelbrot. Fractal theory was established in 1960s. During the empirical fractal analysis for financial time series, the term "econophysics" is used since the fractal analysis methods used for fractal

analysis of financial time series consider the series were originally developed by physicists as outputs of dynamical systems.

Mandelbrot, in 1982, defines fractal theory as a study of roughness. Compared to Euclidian geometry, Fractal geometry is used to work on rough and complex patterns. The most important features of the fractals are self-similarity. As it is mentioned before there are many examples of self-similar cases in nature that we can exhibit. Another important feature of fractal geometry which differentiates it from Euclidian geometry is non-integer dimensions. To be able to understand the fractal structure of an object, scientists look at them at different scales to find self-similarity. These self-similarities are generally expressed as scaling laws.

The definition of scaling law is described by Kantelhardt in (Kantelhardt 2008, p. 3) as follows:

Definition 1.1 (Scaling Law): *Scaling law is a power law with scaling exponent (e.g. α) describing the behaviour of a quantity F as a function of scale parameters s at least asymptotically: $F(s) \sim s^{\alpha}$. The power law should be valid for a large range of s values, e.g., for at least one order of magnitude.*

In the light of this definition, Fractal systems can be described as follows:

Definition 1.2 (Fractal System): *If a system can be characterized by a scaling law with non-integer scaling exponent α , it can be said that this system behaves like fractals.*

Up to now, we have concentrated on mono-fractal structure and general properties on fractal geometry. Although, the notion of fractals seems to be hard to understand, they are not complicated as is thought since they can be described by a single scaling exponent. There are multifractal systems or time series whose properties cannot be described by a single scaling exponent but by a function of scaling exponents. It is known that scaling systems seem to be generally multifractal.Monofractal methods can measure only one fractal dimension characterizing the given time series. This is suitable for those time series which have the same scaling properties throughout.Monofractal and multifractal structures of time series are particular kinds of scale invariant structures. In general, the monofractal structure of time series is expressed by a single power law exponent (Hurst (or Hölder) exponent) and it is assumed that the scale invariance is independent of both time and space.

However, spatial and temporal variations in scale invariant structure of biomedical signals often appear. These spatial and temporal variations show a multifractal structure of the time series that is defined by a multifractal spectrum of power law exponents.

The financial markets, especially stock market indices, are in fact inhomogeneous, which leads to the idea that different parts of the data have different scaling properties. This result leads us to the multifractal analysis of financial time series, more specifically, stock market indices.

The easiest way of multifractal analysis that has been built up stands on the standard partition function multifractal formalism which is called multifractal random walk (Rosenstein, Collins, De Luca, 1992). This method is a highly efficient formalism for the multifractal characterization of normalized and stationary measures. Unfortunately, it does not give the correct result for nonstationary time series. Kantelhardt introduced multifractal detrended fluctuation analysis (MF-DFA) for the multifractal characterization of nonstationary time series. This approach is based on a generalization of the DFA method. As a remarkably powerful technique, MF-DFA has so far been applied to various fields of stochastic analysis, for instance, in markets return analysis, in geophysics, in biophysics, and also in various branches of basic and applied physics.

Multifractal Detrended Fluctuation Analysis (MF-DFA) is based on the identification of scaling of the q'th-order moments' power-law dependence on the signal length and is a generalization of the standard DFA which uses only the second moment$q = 2$.

The other method to discover the multifractality, more specifically self-similarity property of fractal geometry, in financial time series is the Wavelet Transform Modulus Maxima (WTMM).This method relies on the detection of scaling of the maxima lines of the continuous wavelet transform on different scales in the time-scale plane. This procedure is assumed to be especially suitable for analyzing non-stationary time series.

In monofractal cases, there are methods to find the fractal dimension of a given dynamical system or time series. Rescaled Range (R/S) is the first method that we are going to present in the theory part. This method allows us to determine the scaling exponent of a system or time series and the exponent that extracted from this analysis is called as "Hurst" exponent. The details of (R/S) analysis are given in the theory section. There are two methods for finding the fractal dimensions of dynamical systems namely Higuchi and Katz methods.

These two methods have linear relationships between Hurst exponent and these are going to be found in the next section. Another method to find scaling properties of time series is Detrended Fluctuation Analysis (DFA) and it generates the main idea of MF-DFA. In other worlds, MF-DFA is the generalization of DFA. We also interested in frequency domain of stock market indices using well-known Fourier Transform or power spectrum analysis. Finally, we use the TISEAN package to find the Lyapunov exponent, delay time and embedding dimension of the investigated indices to analyze possible chaotic behavior.

For multifractal analysis, as we mentioned above, we use WTMM and MF-DFA and details about both of this methods is presented in the second part of the theory section.

Organization of parts of this thesis planned as follows: In the second section, we present the algorithms for both monofractal and multifractal methods in detail. In the third section, results of the fractal analysis of the stock market indices are given. We use different data sets in the same period from 1st January 2005 to 1st January 2015. In last part, we end up the discussion with a conclusion.

2. THEORY

2.1. Monofractal Methods

2.1.1. Rescaled Range Analysis

Rescaled range analysis (R/S) was developed by Harold E. Hurst when he was working on the Nile River Dam Project in Egypt.After his work the technique was applied to financial time series by Mandelbrot and van Ness.

R/S analysis is a simple process which is highly data-intensive. To be able to understand R/S analysis, it is reasonable to follow the given sequential steps one by one below:

- Start with a time series of length of N. Then convert this time series to a time series with length $\boldsymbol{N' = (N - 1)}$ with the following logarithmic ratios:

$$N_i' = \log(\frac{N_{i+1}}{N_i}) \tag{2.1}$$

- Then divide this generated time series into M number of adjacent sub-periods of length m, satisfying the following condition $M * m = N$. Then give a name to each sub-period $I_a$where $a = 1, 2, 3 \dots M$. Each element in sub-periodI_a can be named as $N_{k,a}$where $k = 1,2, \dots . m$. For every I_a of length m the average value $e_a$is defined as:

$$e_a = \frac{1}{m}\sum_{k=1}^{m} N_{k,a}'. \tag{2.2}$$

The time series of accumulated departures X from the mean value $e_a$for each I $_a$ is

$$X_{k,a} = \sum_{i=1}^{k}(N_{i,a}' - e_a). \tag{2.3}$$

- The range is defined for each sub-period $I_a$as:

$$R_{I_a} = \max\left(X_{k,a}\right) - \min\left(X_{k,a}\right) \tag{2.4}$$

$$k = 1,2,3, \dots, m.$$

- The standard deviation for each sub-period I_a can be calculated by:

$$S_{I_a} = \sqrt{\frac{1}{m}\sum_k \left(N'_{k,a} - e_a\right)^2}. \quad (2.5)$$

- Each range can be normalized by dividing it byS_{I_a}. Then the rescaled range for each is equal to R_{I_a}/S_{I_a}. We have adjacent M sub-periods of length m. Then, the average R/S value of length m is:

$$(R/S)_m = \frac{1}{M}\sum_{a=1}^{M}(R_{I_a}/S_{I_a}). \quad (2.6)$$

- The length m is increased to the next higher value such that (N-1)/m is an integer value. We use values of m that includes start and final points of the time series and steps given above are repeated until m=(N-1)/2.Then we can apply least squares regression on log(m) vs. $\log\left(\frac{\mathrm{R}}{\mathrm{S}}\right)_{\mathrm{m}}$ as:

$$\log(\frac{R_m}{S_m}) = \log c + H * \log m. \quad (2.7)$$

Note that R/S is the ratio of two different measures of dispersion, range and standard deviation. By these steps we calculate H, the Hurst Exponent. The Hurst exponent has a very close relationship to the fractal dimension. The following linear relation holds:

$$D = 2 - H \quad (2.8)$$

where D is the fractal dimension. Using the Hurst exponent we can classify time series into types and gain some insight into their dynamics.

A value H in the range $0.5-1.0$ indicates a time series with long-term positive autocorrelation, meaning both that a high value in the series will probably be followed by another high value and that the values a long time into the future will also tend to be high. A value in the range $0 < H < 0.5$ indicates a time series with long-term switching between high and low values in adjacent pairs, meaning that a single high value will probably be followed by a low value and that the value after that will tend to be high, with this tendency to switch between high and low values lasting a long time into the future. A value of $H = 0.5$ can indicate a completely uncorrelated series, but in fact it is the value applicable to series for which the autocorrelations at small time lags can be positive or

negative but where the absolute values of the autocorrelations quickly decay exponentially to zero.

2.1.2. Detrended Fluctuation Analysis

The detrended fluctuation analysis (DFA) algorithm is a scaling analysis method used to estimate long-range temporal correlations of power-law form (Peng et al.1995), (Hardstone et al., 2012). Its advantage is the fact that extreme values are less likely to affect the result. DFA can be applied by the following four steps**:**

- Firstly, we need to determine the "profile" of the time series X_i of length N (where i=1..N) ($Y(i)$):

$$Y(i) = \sum_{i=1}^{k}(X_i - \bar{X}) \tag{2.9}$$

  where$\overline{X}$ is mean of the time series.
- In the second, step profile $Y(i)$ is divided into non-overlapping segments of length l where the number of segments is the integer $N_l = int(\frac{N}{l})$. At the end of this procedure the short part of the time series would remain. To overcome this problem, the second step can be repeated from the end of the time series. That's why,$2N_l$ segments are generated.
- In the third step for each segment the local trend is calculated using least-squares fitting.

$$F^2(t) = \frac{1}{l}\sum_{i=1}^{l}\left[Y\big((\nu-1)t+i\big) - p_\nu(i)\right]^2 \tag{2.10}$$

  For each segment ν, $\nu = 1,2,\dots,N_l$ and $p_\nu(i)$ is a fitting polynomials for each segment.

- The final step is finding the average over all segments and taking the square root to get the fluctuation function $F(l)$:
-

$$F(l) = \sqrt{\frac{1}{2N_l}\sum_{\nu=1}^{2N_l} F_t^2(\nu)} \tag{2.11}$$

If the data are long-range power-law correlated, $F(l)$ increases, for large values of l, as a power-law:

$$F(l) \sim l^{\alpha} \tag{2.12}$$

where α, the fluctuation exponent can be obtained by finding the slope of the logarithmic graph of $F(l)$ vs. l.

If α is between 0<α<1/2, there is an anti-correlation which means small values are, in general, followed by greater ones. If α=1/2, time series represents Gaussian white noise. If α is in the range 1/2 <α<1, the time series is stationary and there is long-term correlation. If α is greater than 1, there is a correlation other than power law, such as Brownian motion (α=3/2).

2.1.3. Katz Method

Katz's method calculates the fractal dimension of a time series as follows:

- The sum of (Euclidean) distances between the successive points of the time series are calculated as:

$$d = \max\big(distance(1,i)\big). \tag{2.13}$$

- The fractal dimension of the time series is given as:

$$D = \frac{\log_{10} L}{\log_{10} d}. \tag{2.14}$$

The fractal dimension compares the actual number of units that compose a curve with the minimum number of units required to reproduce a pattern of the same spatial extent. Fractal dimensions computed in this fashion depend upon the measurement units used. If the units are different, then so are these dimensions. Katz's approach solves this problem by creating a general unit or yardstick: the average step or average distance $\underline{a}$ between successive points.

$$D = \frac{\log_{10} \frac{L}{\underline{a}}}{\log_{10} \frac{d}{\underline{a}}} \tag{2.15}$$

If we define n as the number of steps in the curve then $n = L/a$ and the fractal dimension D is:

$$D = \frac{\log_{10} n}{\log_{10} n + \log_{10} d/L}. \quad (2.16)$$

2.1.4. Higuchi Method

This is a slightly different method for determining fractal dimension. We have the time series $X(i)$ with a length N where i =1... N and the data are taken at regular intervals.

We create the new time series from the given time series$X(i)$:

$$X(m), X(m+k), X(m+2k), \dots, X(m+\left[\frac{N-m}{k}\right].k) \quad (2.17)$$

In this representation m shows the initial time and k indicates the time interval and [ ] represents greatest integer function. By this way, we will have constructed k sets of time series. We can calculate the length of the curve of the constructed time series:

$$L_m(k) = \{(\sum_{i=1}^{\frac{N-m}{k}} |X(m+ik) - X(m+(i-1)k)|) \frac{N-1}{\left[\frac{N-m}{k}\right].k}\}/k. \quad (2.18)$$

The average length of the curve $< L(k) >$is defined as:

$$< L(k) > = \frac{1}{k} \sum_{m=1}^{k} L_m(k) \quad (2.19)$$

If the curve has fractal behavior L(k) has a power law behavior:

$$< L(k) > \sim k^{-D} \quad (2.20)$$

We can get the fractal dimension D from the slope of the best fitted line corresponding to the plot of $\log(< L(k) >)$ against log (k).

2.1.6. Power (Fourier) Spectral Analysis

The purpose of spectral analysis is to study the properties of an economic variable over the frequency spectrum, i.e. in the frequency-domain. In particular, the estimation of the population spectrum or the so-called power spectrum (also known as the energy-density spectrum) aims at describing how the variance of the variable under investigation can be split into a variety of frequency components. (Masset, 2008). A deterministic signal has few Fourier components; signals coming from a non-deterministic process have many frequencies.

In Fourier analysis, the given time series (or signal) is demonstrated as a family of sinusoidal functions. In Fourier transform, the time series $X(t)$ converted to "frequency-domain" representation $X(t)$.The set of values $X(t)$ for each frequency f is called as spectrumof (t).

The Fourier Spectrum can be calculated mathematically as follows:

$$X(f) = \int_{-\infty}^{\infty} X(t)e^{2\pi ift}\, dt \tag{2.21}$$

2.1.7. Estimation of Lyapunov Exponents from Experimental Data

Experimental data generally is composed of discrete measurement of a single observable. An attractor can be reconstructed using its phase space with delay coordinates; whose Lyapunov spectrum is similar to that of the original one. The delay coordinates contains information about other coordinates, because its Taylor expansion is:

$$x_i(t + \Delta t) = x_i(t) + \Delta t \sum_{j=1}^{N} \frac{\partial x_i(t_0)}{\partial x_j} \frac{dx_j(t)}{dt} + \cdots \tag{2.22}$$

Note that $\frac{dx_j}{dt}$ $, j \neq i$ is implicity involved in this expansion. Obviously, there is no prior knowledge about the dimensionality of the system. That's why there is uncertainty in the number of delay coordinates. This raises two important problems: The first problem is reconstruction of the attractor and the second problem is calculation of Lyapunov spectrum. The latter problem can be solved using Wolf algorithm which is used to estimate

non-negative Lyapunov exponents from reconstructed attractor examining orbital divergence length scales that are always as small as possible, using an approximate GSR (Gram Schmidt Reduction) procedure in the reconstructed phase space as necessary.

To estimate Lyapunov exponent λ, the long-term evolution of a single pair of nearby orbits is followed. The attractor which is reconstructed will supply points to define state of the first principal axis whose spatial dimension is small. When the separation of nearby orbits becomes large, GSR is used on the vector which they define.
This procedure requires replication of the non-fiducial data points with a point nearby the fiducial point, in the same orientation as the original vector. Through this replacement which aims to preserve the orientation and also minimize the size of replacement vector, the long-term behavior of a single principal axis vector is observed. Each replacement vector would be evolved until a problem happens because of overflow or underflow. This allows us to estimate Lyapunov exponent λ (Wolf et al., 1985), (Takens, 1980).

This procedure could be extended to many non-negative exponents as needed, if one cares to estimate: k+1 points in the reconstructed attractor space. Define a k-volume element whose long-term evolution is possible through a data replacement procedure that aims to protect phase space orientation and probes only the small scale structure of the attractor. The growth rate of a k-volume element provides an estimate of the sum of the first *k* Lyapunov exponents.
The algorithm that is mentioned above can be constructed as follows:
Given a time series $x(t)$, an-dimensional phase portrait can be constructed with delay coordinates i.e., a point on the attractor is $\{x(t), x(t+\tau), \ldots., x(t+[n-1]\tau)\}$ where τ is the delay time (Wolf et al., 1985), (Takens, 1980).$L(t_0)$is the distance between the initial point and the nearest neighbor to the initial point $\{x(t_0), \ldots., x(t_0+[n-1]\tau)\}$ .At a later instant this distance evolves to $L'(t_1)$.The distance is propagated through the attractor for a time short enough so that only small scale attractor structure is likely to be examined.If the evolution time is too large we may see L' shrink as the two trajectories which define it pass through a folding region of the attractor. This will result in the under estimation of the Lyapunov exponent λ.In that case, we need to find for a new candidate point where both the separation from the evolved fiducial point and the angular separation between the

evolved and replacement element are small. This cycle is repeated until the fiducial trajectory spans the entire data file and so we can estimate the Lyapunov exponent as follows:

$$\lambda = \frac{1}{t_N - t_0} \sum_{k=1}^{N} \frac{L'(t_k)}{L'(t_{k-1})} \tag{2.23}$$

where$N$ is the total number of replacement steps.

To be able to accurately estimate Lyapunov exponents, we need to give great care in choosing two parameters namely embedding dimension and delay time. Let us have a scalar time series $\{x(t_i)\}, t_i = t_0 + i\Delta t$, which is obtained by sampling with period Δt of the coordinates of state vector $f_t(x) \in R^n$.After that there exist an embedding between the attractor A and the set of n-dimensional vectors (reconstructed attractor) given by:

$$\dot{x}(t_i) = [x(t_i), x(t_i + \tau), \ldots\ldots, x(t + (m-1)\tau)]^{\tau} \tag{2.24}$$

if$n$ and τ satisfy at least the following conditions:(Takens,1980):

- An embedding is a smooth, one to one coordinate transformation with a smooth inverse. (Kostelich and Swinney,1989).
- If τ is too small then all coordinates of a vector $\dot{x}(t_i)$ will be nearly equal, and the reconstructed attractor will lie close to the diagonal. If τ is too large, the coordinates of the vector $\dot{x}(t_i)$ will be decorrelated, and the structure of the attractor A will not be reproduced by the reconstructed attractor.

2.2. Multifractal Methods

2.2.1. MF-DFA(Multifractal Detrented Fluctuation Analysis)

Although the structure of both monofractal and multifractal time series are not the same, they have similar RMS (Root Mean Square) and Hurst (or Hölder) exponents. The multifractal time series have both extremely small and large local fluctuations which result in a normal distribution for the monofractal time series where the variance is calculated by the second order statistical moment alone.

The aim of the MF-DFA is to find the spectrum of singularities both for stationary and nonstationary time series. MF-DFA is obtained by q-order extension of the overall RMS and the power law relation between q-order RMS is numerically expressed by the q-order Hurst exponent $H(q)$. (Ihlen, 2012)

The MF-DFA procedure can be expressed by the following 5 steps:

- Suppose we have the time series x_k with length N. Firstly, we need to determine the profile $Y(i)$ of time series x_k :

$$Y(i) = \sum_{k=1}^{i}(x_k - \overline{x}),\ i = 1, \dots, N \tag{2.25}$$

where$\overline{x}$ is the mean of the time series. Secondly, the profile $Y(i)$is divided into

$N_s \approx int(\frac{N}{s})$non-overlapping segments of length s.Since the length N of the series is often not a multiple of the considered time scale, a short part at the end of the profile may remain. In order to include this remaining part of the time series, the same procedure is repeated starting from the opposite end of the time series. At the end of this procedure, we have a total of $2N_s$ segments.

- Thirdly, we need to detrend the generated profile $Y(i)$ for each segment with length s. To be able to do this, we need to find the local trend for each of $2N_s$ segments by the least-square fit of the time series and determine the variance:

$$F^2(s,v) = \frac{1}{s}\sum_{i=1}^{s}\{Y[(v-1)s+i] - w_v(i)\}^2 \ \ for\ each\ segment\ v, v = 1, \dots., N_s.$$

For segments $v = N_s + 1, \dots.,2N_s$, the variance is defined as:

$$F^2(s,v) = \frac{1}{s}\sum_{i=1}^{s}\{Y[N-(v-N_s)s+i] - w_v(i)\}^2 \tag{2.26}$$

where$w_v(i)$ is the fitting polynomial of order m for the segment,v. The degree of the fitting polynomial can be linear, quadratic, cubic, or higher order. (Conventionally called DFA1, DFA2, DFA3,...). Since the detrending of the time series is done by the subtraction

of the polynomial fits from the profile, different order DFA's differ in their capability of eliminating trends in the series.

- In the fourth step, to be able to get the q-order fluctuation, we need to take the average of the variances for each of the segments v:

$$F_q(s) = \left[\frac{1}{2N_s}\sum_{v=1}^{2N_s}[F^2(s,v)]^{\frac{q}{2}}\right]^{\frac{1}{q}} \tag{2.27}$$

where order q can take any real value other than zero. It can also be noted that for q=2, the standard DFA procedure is generated. Since we are interested in how the generalized q dependent fluctuation functions $F_q(s)$ depend on the time scales for different values of q, the procedure in steps 2 to 4 should be repeated for several time scales s. It is obvious that $F_q(s)$ is going to increase as the time scale increases.

- In the final step, the scaling behavior of fluctuations is examined by analyzing the log-log plot of $F_q(s)$ vs s. The slope of the plot is going to give the q-order generalized Hurst (or Hölder) exponent $H(q)$.

If small and large fluctuations scale differently, it is possible to see an important dependence of $H(q)$ on q such that for positive values of q, the segment v with variance $F^2(s,v)$ can dominate the average fluctuation. That's why, for the positive choice of q, $H(q)$ represents scaling behavior of large fluctuations and it is also seen that large fluctuations gives small $H(q)$ for multifractal time series. On the other hand, for small values of q, the scaling behavior of segments with small fluctuations can be determined and scaling behavior of small fluctuations are represented with large Hurst exponents $H(q)$.

For stationary, normalized records with compact support, the multifractal scaling exponents $H(q)$ are directly related to the Renyi (or scaling) exponents $\tau(q)$ defined by the standard partition function-based multifractal formalism.

The analytical relation between Renyi exponent $\tau(q)$ and Hölder exponent $H(q)$ is:

$$\tau(q) = qH(q) - 1. \tag{2.28}$$

The Renyi exponent $\tau(q)$ shows transient structure of the time series which means for negative values of q, the scaling behavior of small fluctuations dominates and for large values of q, scaling behavior of large fluctuations can be estimated. If the relation between Renyi exponent and q is nonlinear, the time series can be classified as a multifractal one.

It should be clearly stated that the Hölder exponent $H(q)$ is not the generalized multifractal dimension. The generalized multifractal dimension is denoted as $D(q)$ and defined as follows:

$$D(q) \equiv \frac{\tau(q)}{q-1} = \frac{qH(q)-1}{q-1} \tag{2.29}$$

It should be stressed that for monofractal time series $D(q)$ depends on q while $H(q=2)$ is independent of q.

Multifractal time series can also be classified using the singularity spectrum $f(\alpha)$ which is related to the Renyi exponent $\tau(q)$ via the Legendre transform (Kantelhardt, 2002):

$$\alpha = \tau'(q) \; and \; f(\alpha) = q\alpha - \tau(q). \tag{2.30}$$

Here α denotes Hölder exponent and $f(\alpha)$ is the dimension of the subset of the series.

The relation between α and $f(\alpha)$ and that of $f(\alpha)$ to $(q)$is:

$$\alpha = H(q) + qH'(q) \; and \; f(\alpha) = q[\alpha - H(q)] + 1. \tag{2.31}$$

2.2.2. Wavelet Transform Modulus Maxima (WTMM)

The Fourier Transform (FT) is a good method to see what happens in the frequency domain of a time series. However, when we use FT for non-stationary signals, it cannot satisfactorily resolve the periodicity or multi periodicity of the signal so that information about the stationary nature of the signal cannot be obtained. The FT approach has the following two main problems:

- *It is not possible to tell that at which instant rise of the particular frequency exists, when we take the Fourier transform of the whole data set or time series.*
- *The resolution in frequency is limited by the length of window which has to be imposed.*

The first problem can be handled by Short-time Fourier Transform (STFT). STFT is able to give the information about both frequency and time by sliding the window to find a spectrogram. However; STFT does not have a solution for the resolution problem. The origin of the STFT problem comes from the Heisenberg Uncertainty Principle which states that one cannot know what spectral components exist at given instances of time. What can be seen are time intervals during which certain bands of frequencies exist. This situation creates a resolution dilemma. In STFT window functions are used to find stationary parts in non-stationary signals. If in STFT a window function of infinite length is used, it has the same structure and resolution in frequency as the FT approach with no time information. To be able to get quasi stationarity we have to have a short enough window, in which the signal is stationary. The solution to the resolution problem comes from the Wavelet Transform**.**

The wavelet transform was first mentioned by the mathematician Alfred Haar for his doctoral degree in 1909. The wavelet transform is very close to the Fourier transform with a totally different wavelet function$\psi_{(a,b)}$. While the Fourier transform decomposes the signal or time series into sine or cosine functions which are in the Fourier space and hence not localized in time, the wavelet transform generates functions which are localized in both real and Fourier (or frequency) space.

There are two types of wavelet transform: Continuous Wavelet Transform (CWT) and Discrete Wavelet Transform (DWT). CWT was developed as an alternative to STFT to solve the resolution problem.

There are two main differences between CWT and STFT:

- *The Fourier transform of the windowed signal is not taken, and therefore a single peak will be seen corresponding to a sinusoid, negative frequencies are not computed.*
- *The width of the window is changed as the transform is computed for every single spectral component, which is probably the most important characteristic of the wavelet transform.*

CWT is defined by the following formulation:

$$CWT_X^{\psi}(\tau, s) = \psi_x^{\psi}(\tau, s) = \frac{1}{\sqrt{s}} \int x(t)\psi^* \left(\frac{t-\tau}{s}\right) dt. \quad (2.32)$$

Here τ is the translation parameter, s is the scale parameter, $x(t)$ is the processed signal or time series and ψ is the transforming function or "mother wavelet". ($\psi^*$is the complex conjugate of the wavelet.) To be able to understand this definition, it will be good to look at the meaning of the term "mother wavelet" more closely. Wavelet means small wave which refers to a finite length oscillatory window function. "Mother wavelet" is the function with different regions of support derived from one main function. It is important to note that the factor $\frac{1}{\sqrt{s}}$ is required for normalization such that the transformed signal will have the same energy level at different scales.

In both FT and STFT, the frequency domain is always mentioned and for CWT, we have the scale parameter s .The relation between scale and frequency is as follows:

$$scale = 1/frequency$$

Another type of wavelet transform is the Discrete Wavelet Transform (DWT). Although CWT gives very powerful results in terms of the resolution problem, it requires a significant amount of computation time and resources.The discrete wavelet transform (DWT) supplies sufficient information both for analysis and synthesis of the original signal, with an important reduction in the computation time.

The DWT procedure starts with passing this signal (sequence) through a half band digital low pass filter with impulse response h[n]. Filtering a signal corresponds to the mathematical operation of convolution of the signal with the impulse response of the filter. The convolution operation in discrete time is defined as follows:

$$x[n] * h[n] = \sum_{k=-\infty}^{\infty} x[k]h[n-k] \quad (2.33)$$

Half band low pass filtering removes half of the frequencies, which can be interpreted as losing half of the information. Therefore, the resolution is halved after the filtering operation.

In summary, the low pass filtering halves the resolution, but leaves the scale unchanged. The signal is then sub sampled by 2 since half of the number of samples are redundant. This doubles the scale.

$$y[n] = \sum_{k=-\infty}^{\infty} h[k].x[2n-k] \tag{2.34}$$

DWT employs two sets of functions, called scaling functions and wavelet functions, which are associated with low pass and high pass filters, respectively. The original signal x[n] is first passed through a half band high pass filter g[n] and a low pass filter h[n]. After the filtering, half of the samples can be eliminated so the signal can be sub sampled by 2, simply by discarding every other sample. This constitutes one level of decomposition and can mathematically be expressed as follows:

$$y_{high}[k] = \sum_n x[n]g[2k-n] \tag{2.35}$$

$$y_{low}[k] = \sum_n x[n]h[2k-n] \tag{2.36}$$

where$y_{high}[k]$ and $y_{low}[k]$ are the outputs of high pass and low pass filters. In addition to this, the relation between high pass and low pass filters is as follows:

$$g[L-1-n] = (-1)^n h[n] \tag{2.37}$$

where$L$ is the filter length.

The wavelet transform modulus maxima (WTMM) is a method for detecting the fractal dimension of a signal, the WTMM is able to partition the time and scale domain of a signal into fractal dimension regions, and the method is sometimes referred to as a "mathematical microscope" due to its ability to inspect the multi-scale dimensional characteristics of a signal and possibly inform about the sources of these characteristics.

The WTMM uses the continuous wavelet transform and this method is very suitable when analyzing multifractal time series or signals. The WTMM provides the ability to describe scale and time space by the fractal dimension and this is referred to as “skeleton”. Wavelet Skeleton is an aggregate of all Local Maxima Lines (LML) on each scale of the Wavelet coefficient matrix. Skeleton matrix is a scope of all local maxima points that exist on each scale “s”. In general, the skeleton function shows the scalability of the signal. Multifractal

behavior of signal assumes that the signal does not have some decent fractal measure, but is characterized by the scope of fractal measures. In case of monofractal behavior, the scaling exponential function is a line (Puckovs, 2012).

3. OBSERVATIONAL RESULTS AND ANALYSIS OF STOCK MARKET INDICES

3.1. Monofractal Analysis Results

We use the following data sets for our experimental evaluations: BIST 100 index, BIST 50 Index, BIST 30 Index, Dow-Jones 30 Industrial Index. All the data sets are between the dates 2005-2015 each of which consists of 2516 data points.

In Table 1, the results of fractal dimension calculations according to Katz's and Higuchi's methods are presented. In addition to this, corresponding Hurst exponents are given. When we compare this result to those for the Indian stock exchange results presented in (Sammader*et al.*, 2013), we obtain very close results for both Turkish Stock Market Indexes and the Dow-Jones Index. Since the fractal dimensions are between $1 < D < 2$, it can be said that self-similar property of fractal geometry is observed. It is one of the supporting results that Efficient Market Hypothesis does not represent the realistic view of financial time series. When the Hurst exponents calculated by (R/S) method are taken into account all the Hurst exponents are bigger than 0.5. That means this time series are persistent or trend reinforcing series rather than a series where information from the previous step dominates over information from parallel processes, however, all processes scale in similar ways. In other words, long memory structures exist for this time series. Since this time series are persistent, they presents fractional Brownian motion, or biased random walk. However, since the Hurst exponents are not much bigger than 0.5 it can be said that there will be a noise in the given series due to possible seasonal fluctuations (economic, social or political crisis).

Table 3.1.Fractal Dimensions and Hurst Exponents.

Data Set	Higuchi Method	Katz Method	Hurst Exponent
BIST 100	1.4647	1.6886	0.5951
BIST 50	1.4694	1.7075	0.6368
BIST 30	1.4694	1.7075	0.6368
Dow Jones 30 Industrial	1.5064	1.7586	0.6386

In Figure 3.1, the graphical representation of the (R/S) analysis is given. In this graph, it can be seen that there is breakdown after the first 1200 days of observation. That means

there would be two different time scales. However, the slope of Turkish Stock Markets is increasing after the breakdown, while the slope of Dow-Jones Index is decreasing which is very similar to the result presented in (Cakar, Aybar, Hacinliyan, Kusbeyzi, 2010).

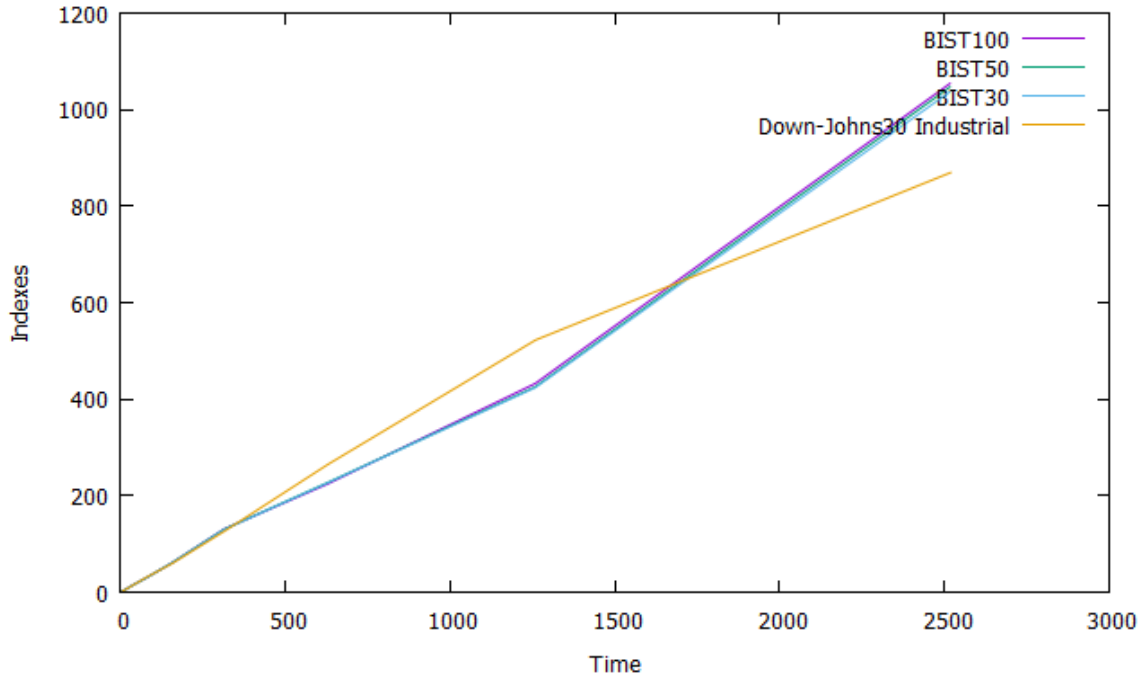

Figure3.1. Rescaled Range(R/S) Analysis of Market Indices

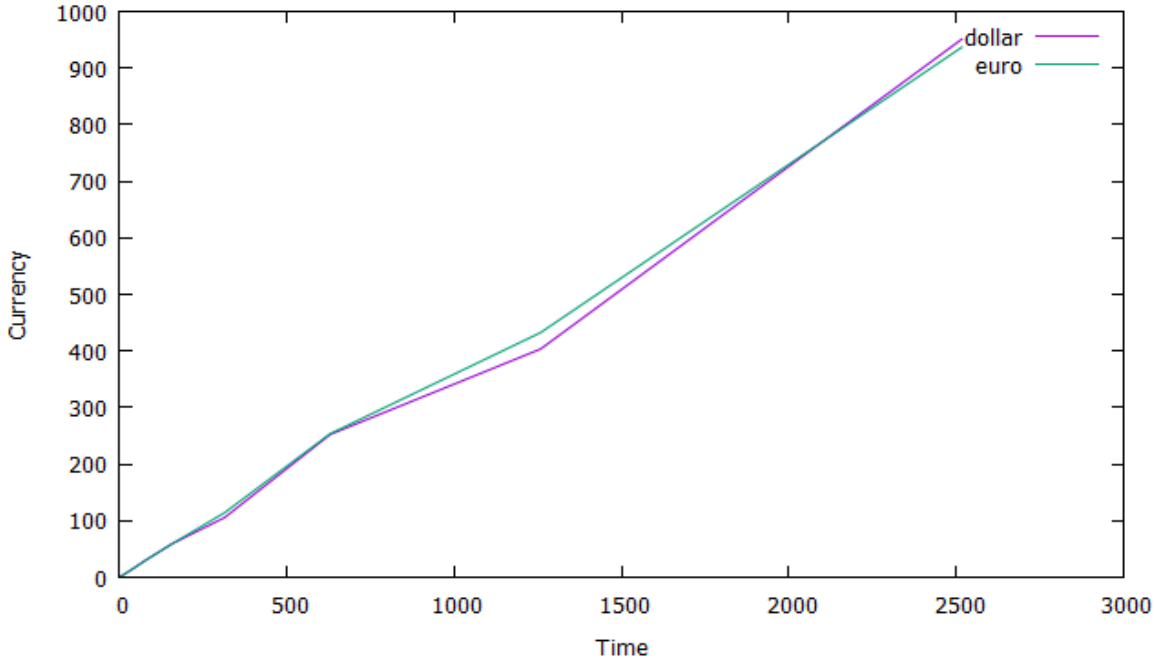

Figure 3.2. (R/S) Analysis of Currency prices

In Figure 3.2, (R/S) analysis of Currency Prices are plotted, for them 3 different time scales are observed and breakdown for both Dollar and Euro are observed in the same instant in this analysis.

The Detrended Fluctuation Analysis results of the given indices, Figure 3.3, shows identical behavior in terms of fluctuation. However, in this analysis two different time scales observedin (R/S) cannot be seen. It is probable that a short term nonstationarity present in the original data has been smoothed out because of the detrending. Therefore, DFA is not a suitable tool to understand the existence of multiple time scales or regimes in this sense, if these trends are due to possible nonstationarity. The same results are observed for the Dollar and Euro prices and their DFA analysis is plotted in Fig3.3. According to DFA analysis both Euro and Dollar follow same trend.

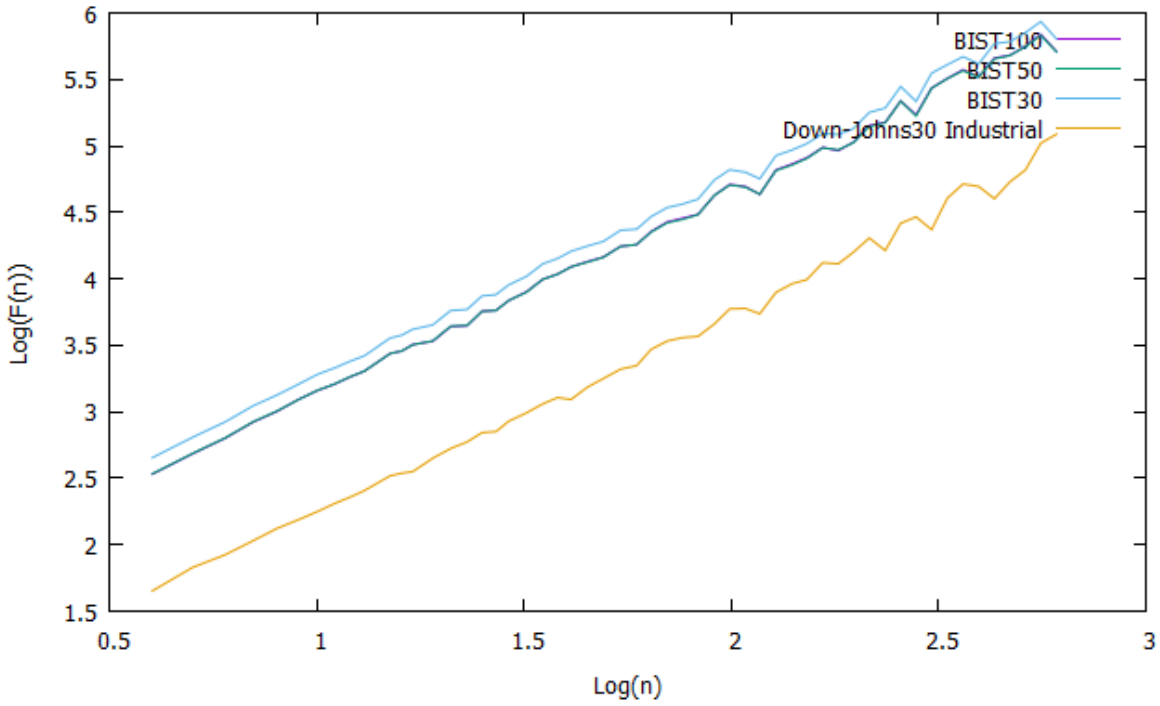

Figure 3.3.Detrented Fluctuation Analysis (DFA) of Stock Market Indices

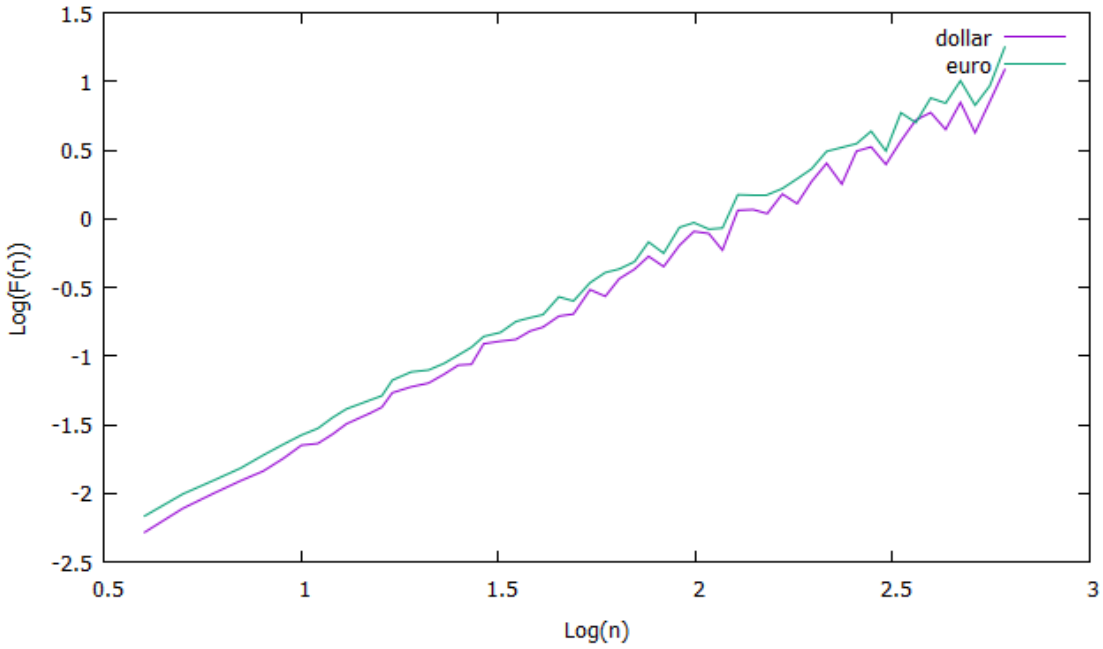

Figure3.4. DFA Analysis of Euro and Dollar Prices

In Figure 3.4, power spectrum of BIST 100 data set versus frequency is plotted in logarithmic scale. The best fit line is $1/f^{1.678}$.(this exponent estimated from f=5 to f=267). This relation which is close to $1/f^2$ implies the Brownian motion as indicated by Hurst analysis.

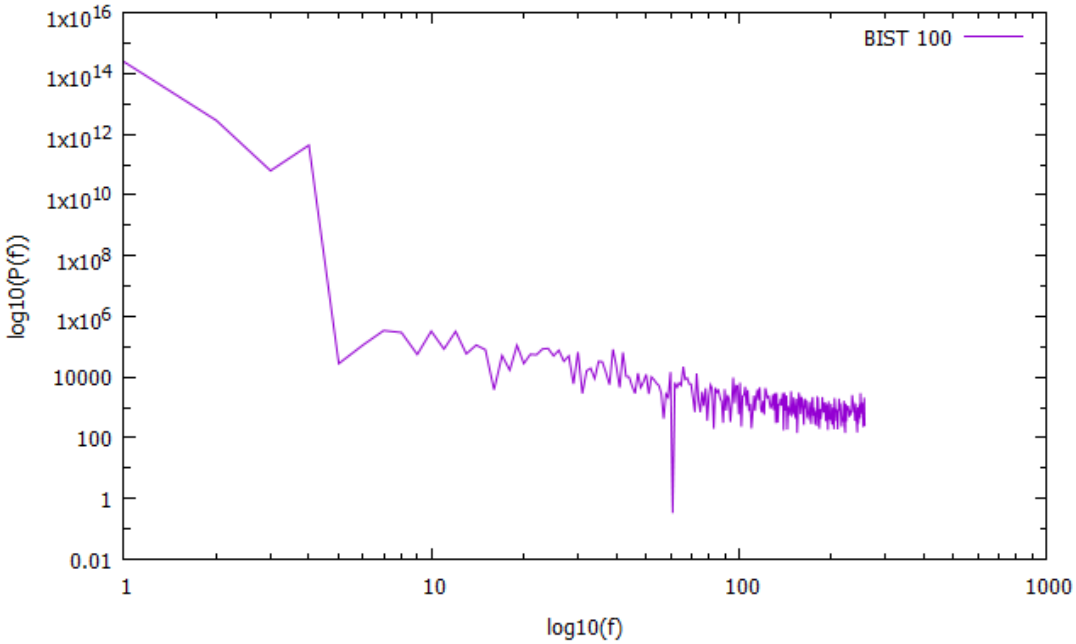

Figure3.5. Power Spectrum Analysis of BIST100 Index

The behavior of the mutual information analysis (Figure 3.4) shows that when all sets of indexes are very close to each other and they have almost the same delay time of 5 days (a week).

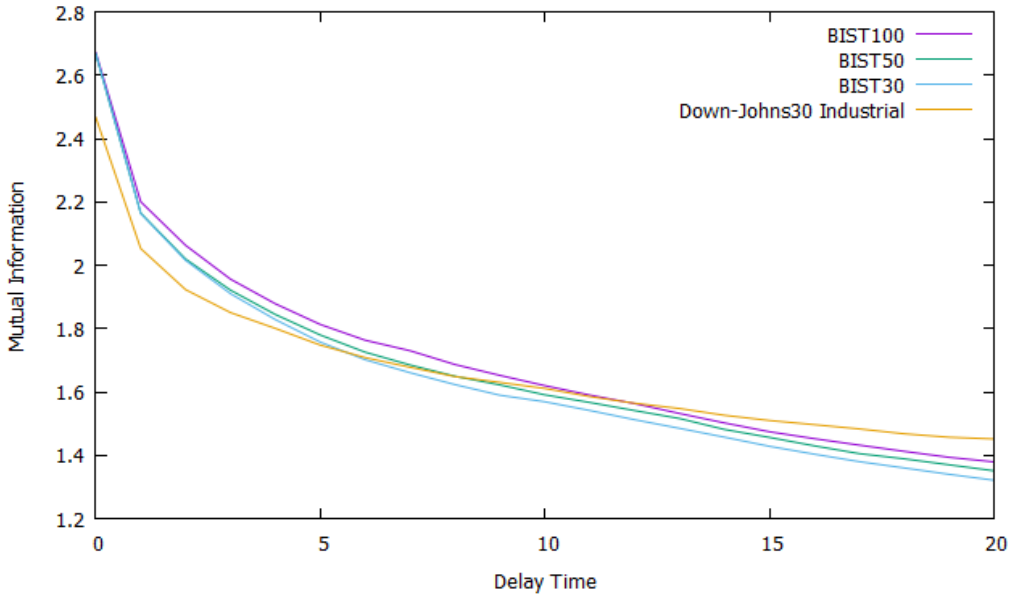

Figure3.6.Mutual Information Analysis of Stock Market Indices

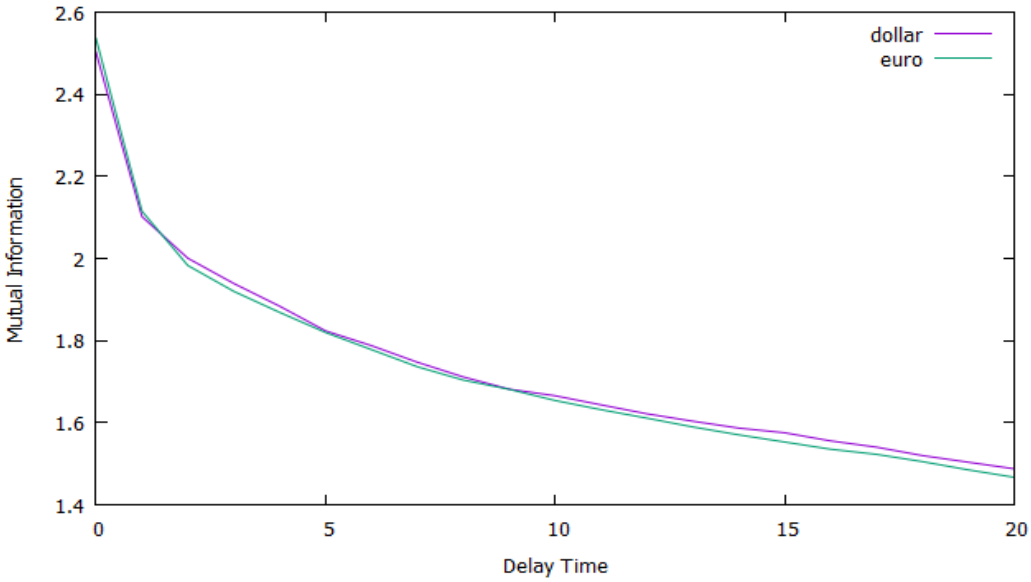

Figure 3.7. Mutual Information Analysis of Currency Prices

The delay time for euro and dollar indices is 5 as in market indices and this is another indicator that currency prices and stock market indices display similar behavior. To be able to understand the meaning of this result we need to mention about the mutual information. Mutual information is one of many quantities that measure how much one random variable

tells us about another. It is dimensionless quantity with (generally) units of bits,and can be thought as the reduction in uncertainty about one random variable given knowledge of another. High mutual information indicates a large reduction in uncertainty; low mutual information indicates a small reduction; and zero mutual information between two random variables means the variables are independent.

After determining delay times, embedding dimensions can be determined. To get a meaningful value for the embedding dimension, false nearest neighbors' method offer a good estimate. After finding delay time for all data sets, the fraction of false nearest neighbors are calculated. The aim of the False Nearest Neighbors (FNN) is to find the number of nearby points. If a small embedding dimension is selected, it will result in false nearest neighbors. The idea behind algorithm of the false nearest as follows:

For each point s_i in the time series look for its nearest neighbor s_j in an n-dimensional space. Calculate the distance $\|s_i - s_j\|$ .Then iterate both points and compute the following:

$$R_i = \frac{|s_{i+1} - s_{j+1}|}{\|s_i - s_j\|} \tag{2.39}$$

If $R_i$exceeds a given heuristic threshold,R_t, this point is marked as having a false nearest neighbor (Kennel, Brown and Abarbanel, 1992). The criterion that the embedding dimension is high enough is that the fraction of points for which $R_i > R_t$ is zero, or at least sufficiently small.

In Figure 3.8, the fraction of false nearest neighbors versus embedding dimension is plotted. All regions embedding dimension graphs' are stabilizing at more than 4 dimensions, implying that at least a two dimensional model is needed.

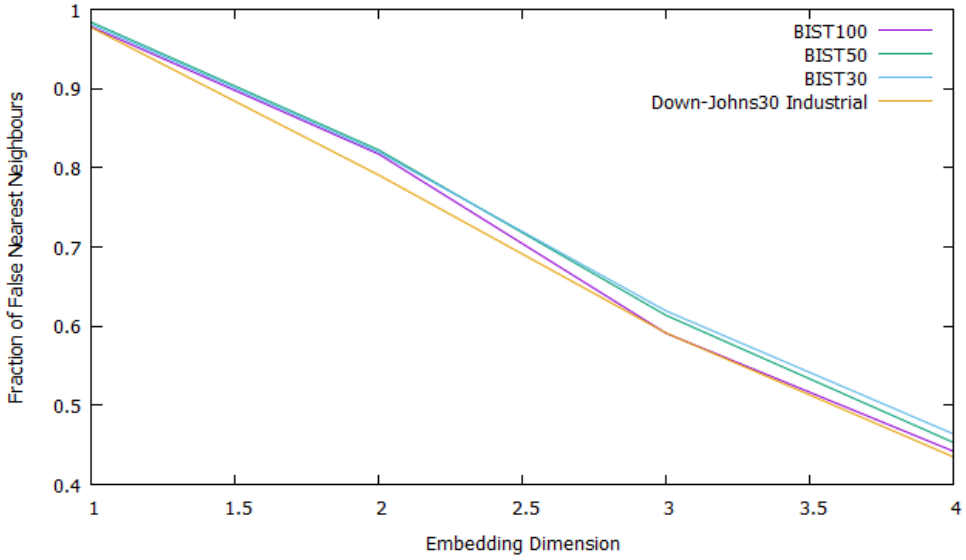

Figure 3.8. False Nearest Neighborhood of Stock Market Indices

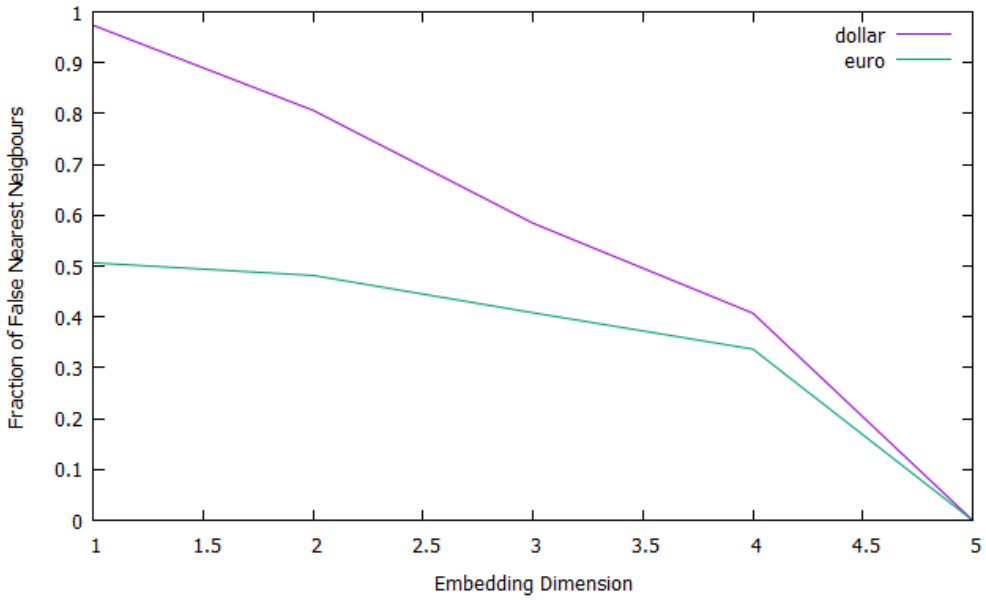

Figure 3.9. False Nearest Neighborhood of Currency Prices

The Lyapunov exponents are invariants of the dynamics. All the slopes in Figure 3.10 are calculated. For BIST 100, Lyapunov exponent is 0.291683±0.0134, for BIST 50 is 0.292167±0.185, for BIST 30 is 0.295938±0.0211 and for Dow-Jones 30 Industrial is 0.26603±0.0187. The standard errors are those coming from the regression. Error propagation is not attempted considering that the data involve exact values of indicesand since we are taking logarithms, parabolic errors will only have significance as an order of magnitude estimate.As a conclusion a positive Lyapunov exponent is indicated from the

studied indices. Since, all Lyapunov exponents are positive, they are not stable fixed points. Consequently, they do not indicate random noise. However, they are positive and this shows that this time series is chaotic.

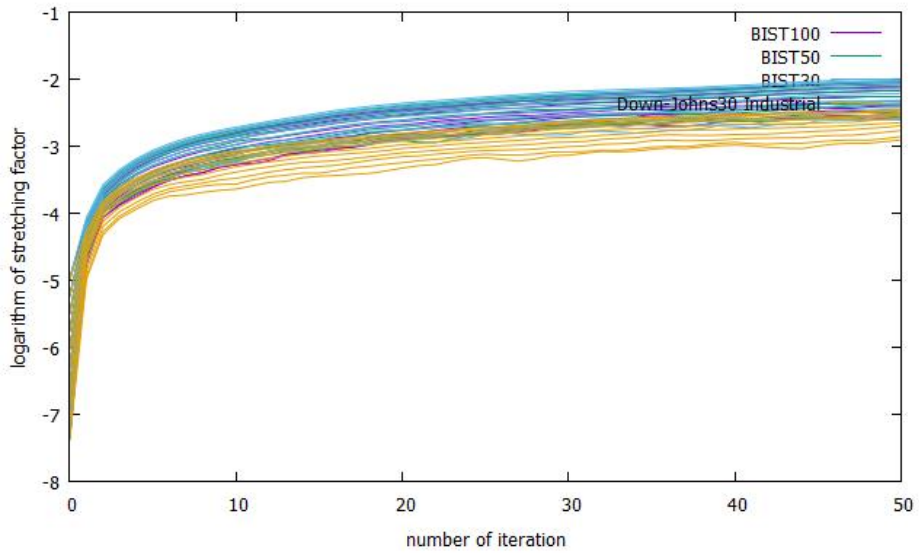

Figure 3.10. Maximum Lyapunov Exponent

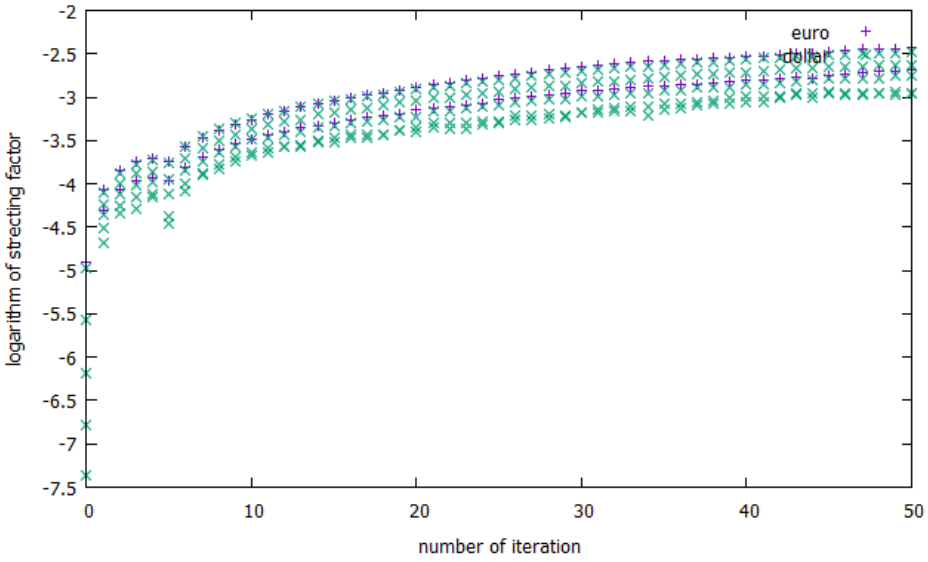

Figure 3.11. Maximum Lyapunov Exponents of Currency Prices

It should be noted that the Lyapunov exponents that we calculate may include error due to two reasons. While calculating Lyapunov exponents we take the logarithmic ratio of the final separation between two nearby trajectories $\delta x_1(t)$as a function of the time where the initial separation of the

trajectories is δx_0.During this calculation, since we use the logarithm, if $\delta x_1/\delta x_0$ is so small, the logarithm of the ratio will tend to diverge. Unless such values can be ignored, calculation of Lyapunov exponents will be somewhat in error. The second reason is the following: Since this method is iterative one, when we calculate the orbit after one iteration it would be reinitialized with new values.

3.2. Multifractal Analysis

We use the same data sets for our multifractal analysis but we restrict ourselves to following two sets: BIST 100 index, Dow-Jones 30 Industrial Index. We apply MFDFA and WTMM analysis to our data sets one by one.

We apply the MFDFA by choosing q order sets from -3 to 3 and scales from 16 to 1024. When the q order varies from $q = -3$to $q = 3$, the q-order Hurst exponent $H(q)$ decreases from 0.6482 to 0.4798. In Table 1 q-order Hurst exponents are presented and in Figure 3.12b H(q) vs. q is plotted. In Figure 3.12a the Fluctuation (scaling) function is plotted .In this figure it can be seen that BIST100 indices show multifractal behavior since for each q order there is a different Hurst exponent $H(q)$ as calculated or in other words, $H(q)$ is not a constant. For $q = 2$ we have the well-known Hurst (or Hölder) exponent $H(q = 2)$ and it is bigger than 0.5 and this gives the idea that there is a positive long-term correlation or memory exists in the series.

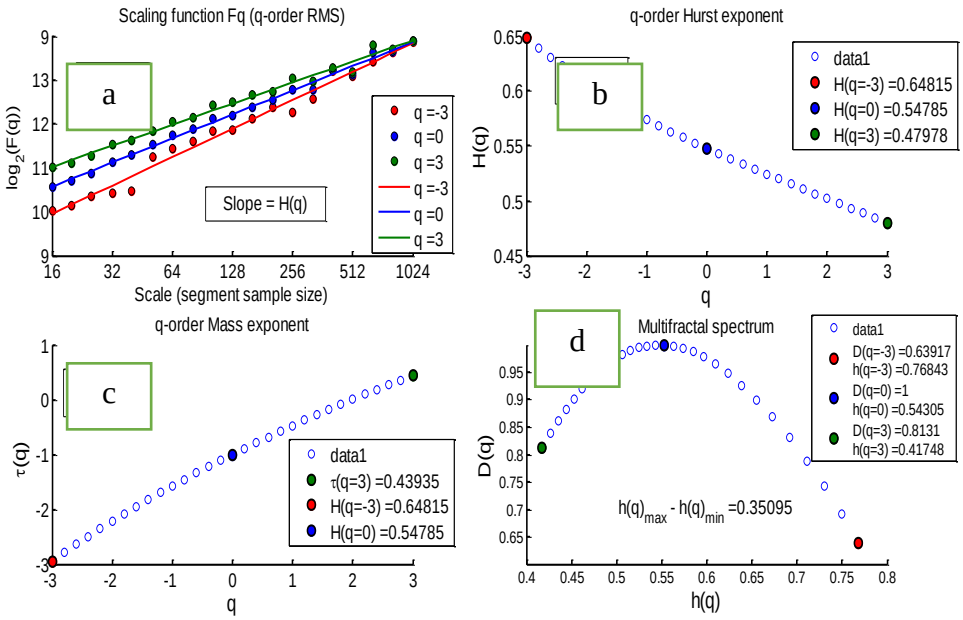

Figure 3.12. MF-DFA Analysis of BIST100 Indices

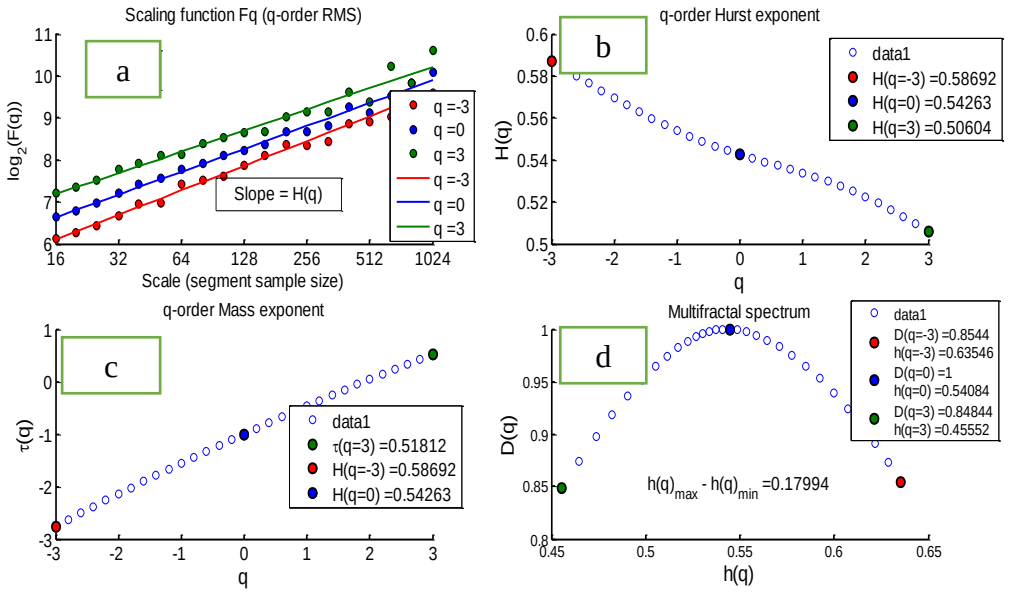

Figure 3.13. MF-DFA Analysis of Dow-Jones 30 Industrial

Table 3.2.q-order Hurst Exponents

H(q)	q=-3	q=-2	q=-1	q=0	q=1	q=2	q=3
BIST 100	0.6482	0.6071	0.5741	0.5479	0.5261	0.5195	0.4798
D-J30 Ind.	0.5869	0.5695	0.5539	0.5426	0.5339	1.5224	0.5060

Table 3.3.q-orderRenyi Exponents

Tau(q)	q=-3	q=-2	q=-1	q=0	q=1	q=2	q=3
BIST 100	-2.9445	-2.6408	-2.6133	-1	-0.4755	0.0417	0.4393
D-J30 Ind	-2.7608	-2.1391	-1.5539	-1	-0.3617	0.0448	0.5181

Another way of understanding the strength of multifractality is looking at the multifractal spectrum. In Figure 3.12d and Figure 3.13d the multifractal spectrum of the two analyzed indices is given. It should be noted that the width of the fractal spectrum indicates strength of multifractal behavior of the signal. If the magnitude $\Delta h(q) = h(q)_{max} - h(q)_{min}$ is large, it indicates much stronger multifractality. The width of the fractal spectrum of

BIST100 is two times bigger than that of the Dow-Jones Industrial 30, showing that BIST100 displays more multifractality than Dow-Jones does. However, $\Delta h = 0.35095$ for BIST100: this means that the multifractal behavior is still not very strong.

Table 3.4.q-order Multifractal Spectrum Exponents

D(q)	q=-3	q=-2	q=-1	q=0	q=1	q=2	q=3
BIST 100	0.6392	0.8682	0.9774	1	0.9729	0.9018	0.8131
D-J30 Ind	0.8544	0.9393	0.9895	1	0.9884	0.9363	0.8484

The continuous wavelet transform of BIST 100 indices shows wavelet coefficients in translation (or time) and scale parameters. Wavelet coefficients matrix is represented in a three-dimensional graph in Figure 3.14b, and it is also represented as wavelet coefficient projection onto the plane formed by the translation and scale parameters as it is implemented in Figure 3.14a. Wavelet coefficients are shown in their absolute values and colored according to their magnitudes. Dark colors represent smaller absolute wavelet coefficient values and light colors indicate larger absolute wavelet coefficient values. The wavelet coefficient matrix allows local maxima lines (LML) selection or Skeleton function construction; LML of BIST is presented in Figure 3.16. The importance of the skeleton Function or LML is that it presents the periodicity of the signal in given scale. In Figure 3.15, the CWT of Dow-Jones 30 Industrial can be found.

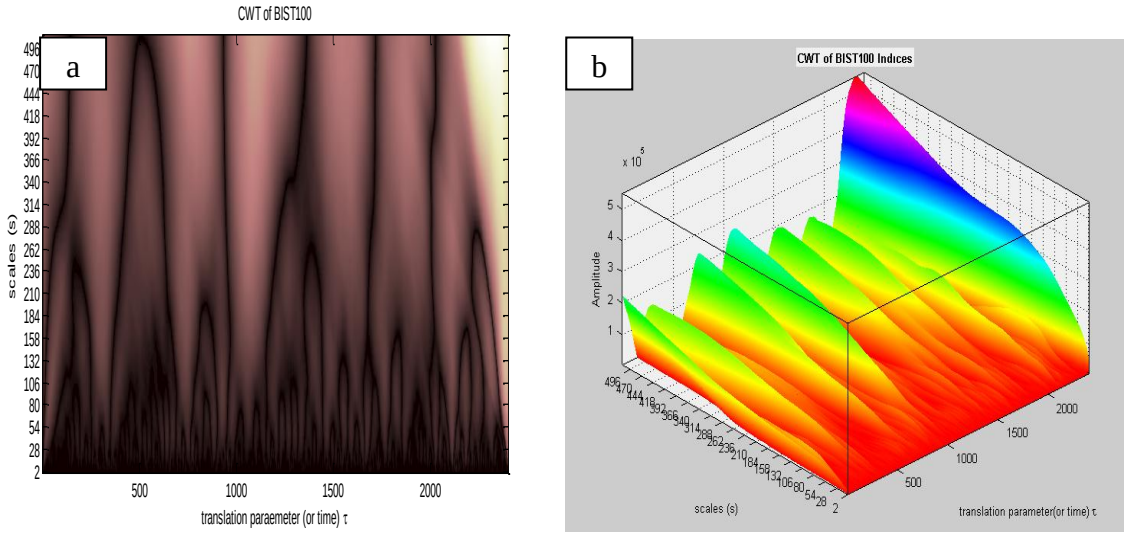

Figure 3.14. Continuous Wavelet Transform of BIST100

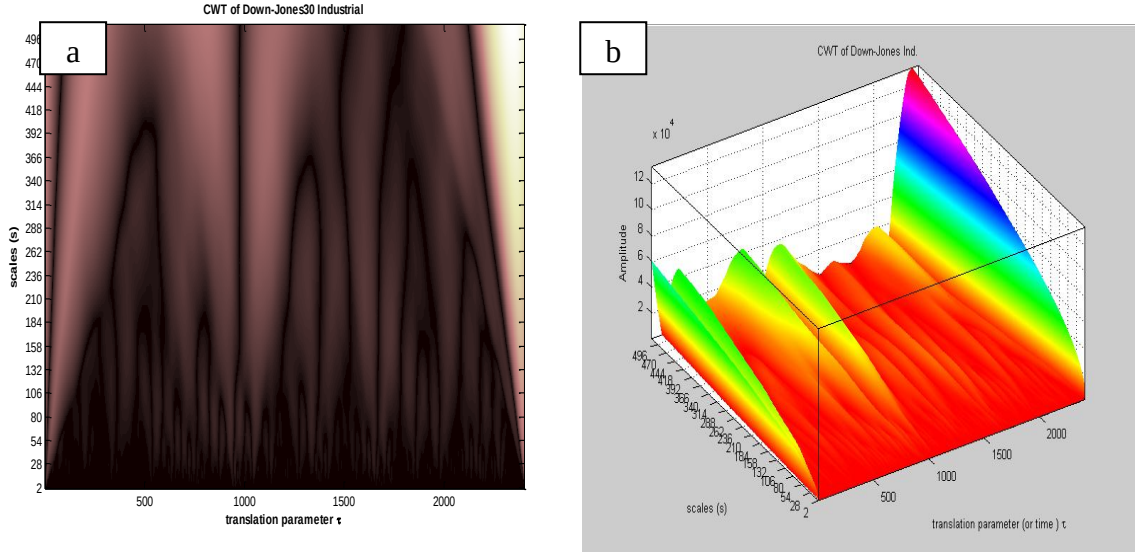

Figure 3.15. Continuous Wavelet Transform of Dow-Jones 30 Industrial

If we want to compare BIST 100 and Dow-Jones 30 Industrial using Figure 3.14b and Figure 3.15b there are more frequency values that affect the behavior of the BIST 100 index than the Dow-Jones 30 Industrial since there are more steep hills in scale and translation parameters space for BIST 100.It should be noted that the mother wavelet function that we use for continuous wavelet transform analysis is:

$$\psi(t) = \begin{cases} 1\,;\ 0 \le t < \frac{1}{2}\,, \\ -1\,;\frac{1}{2} \le t < 1, \\ 0\,;\,otherwise \end{cases} \tag{2.40}$$

Important information related to multifractality of the given time series can be gained by looking at the concavity of the scaling function $\tau(q)$. If it is concave, it can be said that multifractality exists in the time series. In Figure 3.17 and Figure 3.18Renyi exponents for the BIST 100 and Dow-Jones 30 Industrial indices are presented. It can be seen that BIST100 index shows concave behavior while Dow-Jones 30 Industrial looks like convex one so that it can be claimed that multifractal behavior can be more strongly observed in BIST100 index rather than for Dow-Jones 30 Industrial. This result support the intuition

gained from MFDFA analysis for the both indices. However, it should be noted that both time series cannot be claimed to be fully multifractal, since the curves are roughly linear.

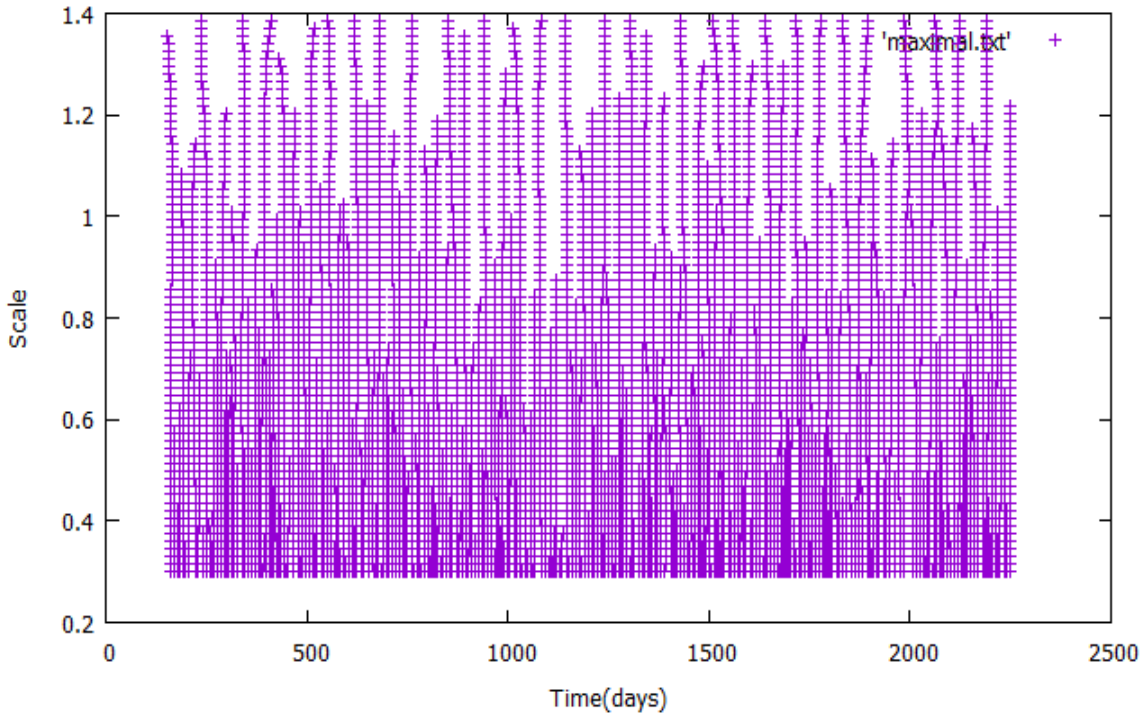

Figure 3.16. Local Maxima Lines of BIST 100

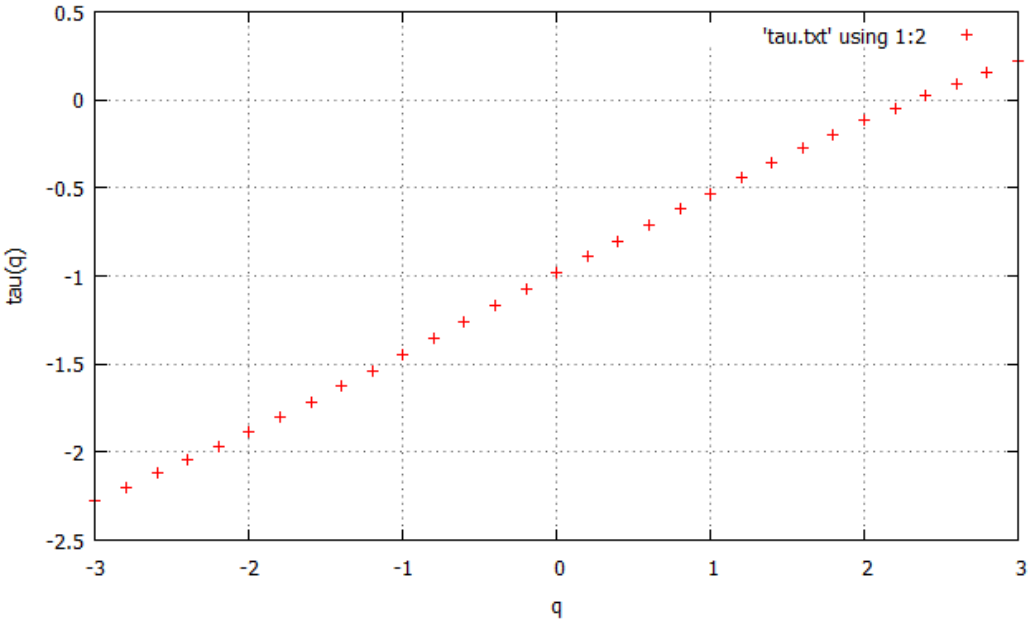

Figure 3.17.q-order Mass (Renyi) exponents of BIST100

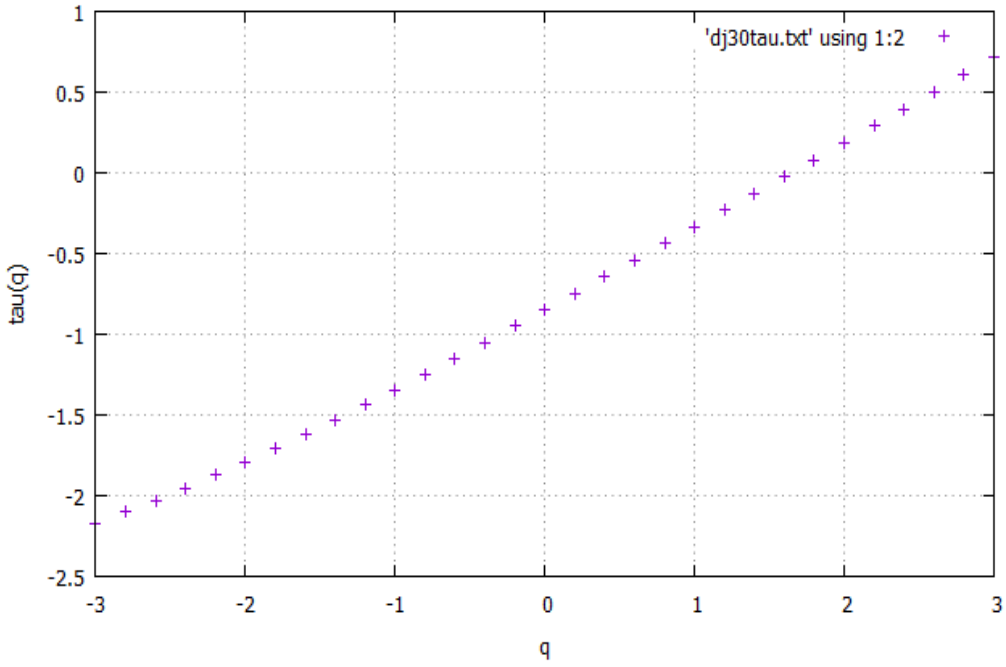

Figure 3.18.q-order Mass (Renyi) Exponents of Dow-Jones 30 Ind.

4. CONCLUSION

All of the stock market data show Fractal Brownian motion trends, meaning that there is a close correlation between each successive step accompanied with positive indicators of chaos. The time period of approximately one week is indicated by three different observations, namely the stabilization of the false nearest neighbors at approximately five periods, Lyapunov exponents around 0.25 indicating a prediction horizon of 3-4 days and disappearance of the two components indicated by Hurst analysis upon detrending. The positive indicators of chaotic behavior are compatible for the findings concerning parallel research in the Indian, Tel Aviv stock markets, dollar and Euro prices and gold prices. ((Sammader*et al*., 2013), (A. S. Hacinliyan *et al., 2010)*, (A. S. Hacinliyan *et al*., 2013), (Alan, İ. KuşbeyziAybar and O.O Aybar, Hacınlıyan, 2013).

In Multifractal analysis using MF-DFA, both BIST 100 and Dow-Jones industrial indices shows multifractal behavior but their power of multifractality is weak. On the other hand, when we use WTMM method, while the same result is obtained for BIST 100 but for Dow-Jones Industrial 30, the multifractality cannot be seen clearly.

APPENDIX A: KATZ FRACTAL DIMENSIONS MATLAB SCRIPT

```
function KFD = katzDimension(signal)
```

```
%      x: Input signal
%      KFD: Fractal Dimension of the input signal
```

```
signal   = signal-mean(signal);
di  = abs(signal(2:end)-signal(1:end-1));
d   = max(abs(signal-signal(1)));
a   = mean(di);
L   = sum(di);
n   = L/a;
KFD = log10(n)/(log10(d/L)+log10(n));
```

APPENDIX B: HIGUCHI FRACTAL DIMENSION MATLAB SCRIPT

```
function xhfd=higuchi(x,kmax)
%function xhfd=hfd(x,kmax)
%Input:
%x: (either column or row) vector of length N
%kmax: maximum value of k
%Output:
%xhfd: Higuchi fractal dimension of x

if ~exist('kmax','var')||isempty(kmax),
    kmax=5;
end;
%%%%%%%%%%%%%%%%%%%%%%%%%%%%%%%%%%%%%%%%%%%%%%%%%%%%%%%%%%%%%%%%%%%%%%%%%%%
x=x(:);
N=length(x);
%%%%%%%%%%%%%%%%%%%%%%%%%%%%%%%%%%%%%%%%%%%%%%%%%%%%%%%%%%%%%%%%%%%%%%%%%%%
Lmk=zeros(kmax,kmax);
for k=1:kmax,
    for m=1:k,
        Lmki=0;
        for i=1:fix((N-m)/k),
            Lmki=Lmki+abs(x(m+i*k)-x(m+(i-1)*k));
        end;
        Ng=(N-1)/(fix((N-m)/k)*k);
        Lmk(m,k)=(Lmki*Ng)/k;
    end;
end;
%%%%%%%%%%%%%%%%%%%%%%%%%%%%%%%%%%%%%%%%%%%%%%%%%%%%%%%%%%%%%%%%%%%%%%%%%%%
Lk=zeros(1,kmax);
for k=1:kmax,
    Lk(1,k)=sum(Lmk(1:k,k))/k;
end;
%%%%%%%%%%%%%%%%%%%%%%%%%%%%%%%%%%%%%%%%%%%%%%%%%%%%%%%%%%%%%%%%%%%%%%%%%%%
lnLk=log(Lk);
lnk=log(1./[1:kmax]);
%%%%%%%%%%%%%%%%%%%%%%%%%%%%%%%%%%%%%%%%%%%%%%%%%%%%%%%%%%%%%%%%%%%%%%%%%%%
b=polyfit(lnk,lnLk,1);
xhfd=b(1);
end
%%%%%%%%%%%%%%%%%%%%%%%%%%%%%%%%%%%%%%%%%%%%%%%%%%%%%%%%%%%%%%%%%%%%%%%%%%%
%%%%%%%%%%%%%%%%%%%%%%%%%%%%%%%%%%%%%%%%%%%%%%%%%%%%%%%%%%%%%%%%%%%%%%%%%%%
%%%%%%%%%%%%%%%%%%%%%%%%%%%%%%%%%%%%%%%%%%%%%%%%%%%%%%%%%%%%%%%%%%%%%%%%%%%
```

REFERENCES

1. Peters, E.P., *Fractal Market Analysis: Applying Chaos Theory to Investment and Economics*, John Wiley & Sons, Inc. New York, N.Y, USA, 1985.
2. Lyapunov exponents", 2015, http://en.wikipedia.org/wiki/Lyapunovexponent, [Accessed March 2015].
3. Rosenstein M.T, J. J. Collins, and C. De Luca, *A Practical Method for Calculating Largest Lyapunov Exponentsfrom Small Data Sets*, 1992.
4. Sammader, Swetadri and Ghosh, Koushik and Basu, Tapasendra , "Fractal Analysis of Prime Indian Stock Market Indices", *International Journal of Bifurcation and Chaos*, Vol.21, No.1, 2013.
5. Li, W.,"Absence of 1/f Spectra in Dow Jones Daily Price", *International Journal of Bifurcation and Chaos 1, Vol. 60,* pp.583-597, 1991.
6. Masset, Philippe, *Analysis of Financial Time-Series Using Fourier and Wavelet Methods*, University of Fribourg, Switzerland, 2008.
7. "Fourier Analysis", 2013, http://research.cs.tamu.edu/prism/lectures/pr/pr_l29.pdf, [Accessed January 2015].
8. Nath, G. C., "Long Memory and Indian Stock Market–an Empirical Evidence.",UTIICM *Conference Paper*, 2001.
9. O. Cakar, O. O. Aybar, A. S. Hacinliyan, I. Kusbeyzi , *Chaoticity in the Time Evolution of Foreign Currency Exchange Rates in Turkey* ,2010.
10. A. S. Hacınlıyan, O. O. Aybar, İ. KuşbeyziAybar, M. Kulalı, Ş. Karaduman, "Signals of Chaotic Behavior in Middle Eastern Stock Exchanges", *Chaos and Complex Systems–Proceedings of the 4th International Interdisciplinary Chaos Symposium*, 2013.

11. Nilufer Alan, İlknurKuşbeyziAybar, O. ÖzgürAybar, Avadis S. Hacınlıyan, “Chaotic Trend Possibility in the Gold Market”, *Chaotic Modeling and Simulation (CMSIM),* 2013.

12. Peng C. K., Havlin S., Stanley H. E., Goldberger A. L.,” Quantification of Scaling Exponents and Crossover Phenomena InNonstationary Heartbeat Time Series”,Cha-*os*, 1995.

13. Hardstone R, Poil S-S, Schiavone G, Jansen R, Nikulin VV, Mansvelder HD and Linkenkaer-Hansen K.,*Detrended Fluctuation Analysis: A Scale-Free View on Neural Oscillations*, 2012.

14. Ihlen, E. A. F.,“Introduction to Multifractal Detrended Fluctuation Analysis in Matlab”,*Frontiers in Physiology*, 2012.

15. W. Kantelhardt, S.A. Zschiegner, E. Koscienlny-Bunde, S. Havlin, *Multifractal Detrended Fluctuation Analysis of Nonstationary Time Series*, 2002.

16. Wolf, A., Swift, J.B., Swinney, H.L., and Vastano, J .A.,*Determining Lyapunov Exponents from a Time Series*, 1985.

17. Takens, F., “Proceedings on Dynamical Systems and Turbulence”, *Lecture Notes in Mathematics*, 1980.

18. B.B. Mandelbrot, *The Fractal Geometry of Nature,* Freeman WH,New York, 1982.

19. Kostelich, E.J., and Swinney, H.L., "Practical Considerations in Estimating Dimension from Time Series Data", *PhysicaScripta*, 1989.

20. M. B. Kennel, R. Brown, and H. D. I. Abarbanel, *Determining Embedding Dimension for Phase-Space Reconstruction Using A Geometrical Construction*, 1992.